Fuel 381 (2025) 133528

Contents lists available at ScienceDirect

Fuel

journal homepage: www.elsevier.com/locate/fuel

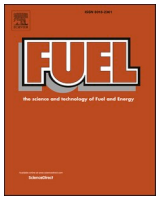

Full Length Article

Evaluating the role of feedstock composition and component interactions on biomass gasification

Mojtaba Ajorloo [a,*], Maryam Ghodrat [a,*], Jason Scott [b], Vladimir Strezov [c]

[a] School of Engineering and Information Technology, The University of New South Wales, Canberra, ACT 2600, Australia
[b] School of Chemical Engineering, The University of New South Wales, Sydney, NSW 2052, Australia
[c] Department of Earth and Environmental Sciences, Macquarie University, NSW 2109, Australia

ARTICLE INFO

Keywords:
Gasification
Biomass
Cellulose
Hemicellulose
Lignin

ABSTRACT

Biomass gasification offers a solution to waste concerns while generating clean energy. This study examines the gasification of pine sawdust (PS), used ground coffee (UGC), and wheat straw (WS) under identical conditions. The compositions of the biomass samples are determined, and the gasification of individual components (hemicellulose, cellulose, and lignin) are conducted to understand the process' dependency on the biomass characteristics. The results suggest cellulose and cellulose-rich biomass (PS) produces more tar and less hydrogen than lignin and lignin-rich biomass (UGC and WS). High lignin and hemicellulose content leave more char. Gasification of PS, UGC, and WS yields 12.7, 15.7, and 17.2 vol% hydrogen, respectively. Additionally, cellulose, hemicellulose, and lignin gasification yield 10.5, 22.1, and 30.4 vol% hydrogen, respectively. Comparing experimental and theoretical values for the three biomass samples reveals significant differences due to component interactions. Thermogravimetry analysis (TGA) indicates significant degradation interactions between hemicellulose-lignin, cellulose-hemicellulose, and cellulose-lignin. It is concluded that high cellulose content biomass shows more predictable results, while high lignin and hemicellulose biomass increases secondary reactions or interactions, exacerbating predictability. These findings assist in estimating gasification performance for better biomass selection.

1. Introduction

As one of the most efficient thermochemical waste-to-energy conversion technologies, gasification offers a double-benefit approach to solve waste management issues and produce energy from various wastes [1,2]. The importance of efficient waste management technologies will be even more significant with the continually fast growth of the global population, causing larger waste accumulation and energy consumption rates [3]. The efficiency of the process depends on various parameters, such as reactor configuration, operating conditions, gasifying agents, and, particularly, feedstock type and properties [4–6].

Biomass is a substantial energy source and can provide a sustainable feedstock for gasification to generate bio-oil, syngas, and biochar as by-product [7–9]. Seasonal availability, high moisture content, low density and high volume, and low-quality bio-oil can be the main constraints of biomass gasification [10]. Furthermore, inconsistent biomass composition varying from one source to another can be problematic.

While biomass selection is hard due to its high diversity, a wide range of biomass are composed of three components, namely hemicellulose, cellulose, and lignin, irrespective of the sources [11]. The composition of biomass in terms of hemicellulose, with its amorphous structure; cellulose, which has a crystalline structure; and lignin, with its complex crosslinked structure, can determine the efficiency of the process and product yields [12–15].

In recent years, many studies have adopted a particular approach to better understand the fundamentals and mechanisms of biomass conversion by assessing its components separately [16,17]. Almagro-Herrera et al. [18] investigated how the three primary biomass components from various sources influence the kinetics of pyrolysis. Anand et al. [19] examined the thermal decomposition behavior of different biomass types in relation to their composition. Ge et al. [20] explored the kinetics and properties of products released through catalytic pyrolysis of the three major biomass components. Zhang et al. [21] focused on the catalytic gasification of specific biomass components to discern how their properties contribute to increased CO production. Kim et al. [22] utilized a machine learning approach to analyze how gasification

* Corresponding authors.
E-mail addresses: m.ajorloo@unsw.edu.au (M. Ajorloo), m.ghodrat@unsw.edu.au (M. Ghodrat).

https://doi.org/10.1016/j.fuel.2024.133528
Received 11 April 2024; Received in revised form 24 September 2024; Accepted 22 October 2024
Available online 25 October 2024

performance correlates with biomass composition. Pang et al. [23] delved into lignin gasification through reactive molecular dynamics simulations to uncover the reaction mechanism. Samani et al. [24] employed computational fluid dynamics (CFD) to study biomass components gasification. These studies collectively underscore the effectiveness and relevance of this approach in recent years.

Furthermore, examining the thermochemical conversion of individual biomass components provides a valuable means of predicting process outcomes through the analysis of biomass composition. However, potential interactions among these components can result in discrepancies between predicted and actual results [7,12]. While some studies disregard interactions between biomass components [11], significant interactions have been observed in certain studies under pyrolysis conditions. Song et al. [25] identified substantial interactions between cellulose/hemicellulose and cellulose/lignin, leading to notable changes in H_2 yield and gas production rate. Zhang et al. [26] suggested that interactions between cellulose-lignin and hemicellulose-lignin enhance solid-to-gas conversion efficiency and accelerate the Boudouard reaction temperature, attributed to the catalytic effect of lignin char. Zhu et al. [27] reported a significant interaction between cellulose and lignin that impeded the rate of cellulose pyrolysis. Xue et al. [28] demonstrated that in the pyrolysis process, interactions between biomass components can play a crucial role in both volatile-volatile and volatile-char states, resulting in alterations in the distribution of products.

While the pyrolysis of biomass components and their potential interactions have been investigated extensively in pyrolysis-focused studies, the emergence of these interactions under gasification conditions remains largely unexplored. Additionally, there is a notable gap in research regarding the predictability of biomass gasification outcomes based on the performance of individual components. The current study addresses these gaps by investigating the gasification of hemicellulose, cellulose, and lignin to elucidate each component's impact on process efficiency and product yields. Specifically, the compositions of three biomass samples: pine sawdust (PS), used ground coffee (UGC), and wheat straw (WS) were first determined. Using these compositions, the theoretical gasification outcomes were estimated and compared with the actual gasification results for each component. Furthermore, thermoanalytical methods were employed to assess the interactions between biomass components and the influence of feedstock composition. This comprehensive approach provides new insights into the role of individual biomass components and their interactions under gasification conditions, advancing our understanding beyond the existing pyrolysis-focused studies. PS, UGC, and WS were selected in this research because of their distinct compositions of cellulose, hemicellulose, and lignin [29,30]. Analysing the gasification outcomes of these biomass types significantly enhances the understanding of the relationship between biomass composition and gasification efficiency. Furthermore, these biomass sources are of great interest due to their abundance as waste streams, ready availability, and low cost.

Predicting biomass gasification behaviour based on its constituents not only aids in analysing the gasification process but also helps in selecting suitable biomass types or designing blends to attain desired gasification outcomes. This knowledge ultimately leads to substantial savings in both time and resources.

2. Experimental

2.1. Materials

The biomass samples used in this study, PS, UGC, and WS, were purchased from a local supplier. The biomass samples were heated at 105 °C for four hrs to remove moisture. Regarding the composition of employed biomass, the lignin content is determined using 72 % sulphuric acid solution based on the Tappi T222 om-88 method described by Carrier et al. [31]. To determine the extractives, hemicellulose, and cellulose, the method described in a work by Ayeni [32] is employed. Xylan from corn core (Code: X0078, Cas: 9014-63-5), as a representative for hemicellulose, was purchased from Tokyo Chemical Industry, Japan. Microcrystalline cellulose from cotton linters (Cas: 9004-34-6) and alkali lignin (Cas: 8068-05-1) were purchased from Sigma-Aldrich. The cellulose, xylan, and lignin were used as received. The properties of the employed feedstock are presented in Table 1.

2.2. Gasification setup

Gasification experiments were performed in a quartz tube gasifier with a length of 55 cm, an internal diameter of 15 mm, and a wall thickness of 1 mm. A quartz sample holder with a length of 8 cm and width of 8 mm was used to load 300 mg sample for each experiment. Following sample insertion, the system was sealed and purified with nitrogen for 30 min before running the experiment. An electrical furnace (length: 25 cm, heating zone length: 10 cm) with a thermocouple connected to a temperature controller was used to heat the system. As a first step, the gasifier was heated to 150 °C in 5 min and held at this temperature for an additional 5 min. This stage ensures uniform heating and removal of any strongly bonded moisture. The sample was then heated at 20 °C/min to the desired gasification temperature where it was held for 90 min. This duration allows ample time to ensure the full conversion of the feedstock into gasification products (gas, char, and tar).

The downstream end of the quartz tube was packed with quartz wool to capture condensates and tar species generated by the gasification process. Non-condensable gasification products were passed into a gas bubbler filled with water (in an ice bath) to recover additional volatile organic compounds (VOCs). The stream leaving the gas bubbler was collected in a multi-layered Tedlar bag for quantitative analyses using a gas chromatograph (GC). Air was used as the gasifying agent, and the ER was calculated as shown in ref. [35]. Selected experiments were randomly repeated twice to assess the reproducibility and reliability of the system. Each repetition was carried out under identical conditions to maintain consistency in the experimental setup. The results from these repetitions were carefully analyzed and compared to identify any variations or discrepancies. The robustness of the findings were ensured, providing a solid foundation for further analysis and application.

The study here defines gas composition on a dry nitrogen-free volumetric basis and syngas yield per mass of feedstock (GY) as the responses. The yield of tar products was determined by weighing the amount of collected tar. The char yield was determined by the difference between the weight of the sample holder before and after gasification. The gas yield was calculated using Eq. (1) [36]:

$$TotalGas(wt\%) = 100 - Tar(wt\%) - Char(wt\%) \quad (1)$$

2.3. Product analysis

The gas composition of the sample collected in the Tedlar bag was analysed offline by a programmable GC (Shimadzu GC-2010) with a methaniser/flame ionisation detector (FID) and thermal conductivity detector (TCD). The column used was a HP-PlotQ with a length of 30 m,

Table 1
Proximate and ultimate analyses of the used feedstocks on dry basis.

Feedstock	Proximate analysis (wt%, db*)			Ultimate analysis (wt%, db)			
	Volatile matter	Fixed carbon	Ash	C	H	O **	N
PS [33]	81.5	17.8	0.6	46.9	6.1	46.4	0
UGC [29]	76.4	22.7	0.9	53.9	7.1	35.8	2.4
WS [30]	73.5	16.4	10.1	43.0	5.3	40.7	0.6
Cellulose [16]	94.6	5.4	0	42.3	6.1	51.6	0
Xylan [34]	76.8	18.31	0.23	41.47	6.48	52.05	0.01
Lignin[16]	62.3	34.9	2.8	55.3	5.3	35.2	0.1

*db:dry basis ** Determined by difference of C, H, and N.

inner diameter of 0.32 mm, and film thickness of 20 μm. The GC carrier gas was helium at a 20 mL/min. The GC column temperature was initially held at 50 °C for five min and then increased to 220 °C at 10 °C/min where it was kept for 10 min. CO, CO_2, CH_4, C_2H_4, C_2H_6, C_3H_6, C_3H_8, and heavier hydrocarbons (up to C_7) were detected by the methaniser/FID arrangement. The external standard approach was employed to quantify the species.

The thermal decomposition behaviour of biomass and its components was studied by thermogravimetric analysis (TGA) and derivative thermogravimetric (DTG) analysis (Q5000 from TA instruments) under air atmosphere at a flow rate of 20 mL/min. The test was conducted from ambient temperature to 800 °C at a heating rate of 20 °C/min. Sample weight was approximately 15 mg.

3. Results and discussion

3.1. Gasification results

Fig. 1 details the gas compositions from PS, UGC, and WS, gasified at T = 800 °C and ER = 0.15. Fig. 1 also compares these biomass' char, gas, and tar yields. As shown in Fig. 1a., the gas produced from the gasification of PS is composed of 6.8 % CH_4, 33.6 % CO_2, 5.9 % C_nH_m, 41.3 % CO, and 12.7 % H_2. Compared to PS, the gasification of UGC and WS produces more hydrogen and less methane and hydrocarbons, while the concentrations of CO and CO_2 are almost the same. The H_2, CH_4, and C_nH_m concentrations for UGC are 15.7, 5.1 and 5.6 %, respectively. For WS, H_2 is 17.2 %, CH_4 is 3.5, and C_nH_m is 2.1 %. Furthermore, the GY for PS, UGC, and WS are 254, 238, and 276 mL/g, respectively. Concerning the product yields from each biomass, Fig. 1b. indicates that in the gasification process, 49.1 wt% of PS converts to tar, 39.5 wt% goes into non-condensable gases, and 11.5 wt% remains as char in the sample holder. While the gas yields for the other biomass are almost the same as PS, the tar yields of UGC and WS are 42.5 and 37.2 wt%, respectively. Also, the char yield for UGC is 17.1 wt% and 19.5 wt% for WS. Among the studied biomass, WS produces more hydrogen and shows higher gas yield. Also, WS gasification results in less tar compared with PS and UGC. UGC shows higher hydrogen efficiency, however, it also produces higher char yields along with WS.

The differences in gas composition and product yields from the investigated biomasses mainly is attributed to their different biomass composition [37]. Fig. 2 gives information about the composition of cellulose, hemicellulose, and lignin in the investigated PS, UGC, and WS samples. Fig. 2 indicates that the PS is composed of 59 % cellulose, 19 % hemicellulose, and 22 % lignin. For UGC, the lignin is 40 %, cellulose is 10 %, and hemicellulose is 50 %. WS's cellulose, hemicellulose, and lignin are 22, 45, and 33 %, respectively.

Taking the information from Fig. 1 and Fig. 2 into consideration, it can be observed that there may be a correlation between higher hydrogen and char yield with higher lignin and xylan contents of the biomass. In addition, the higher tar yield of PS may be due to its higher cellulose content. To gain more insight regarding this hypothesis, the gasification of biomass components is conducted separately, and the results are compared in Fig. 3.

The cellulose gasification leads to the formation of a gas composed of 46.3 % CO, 4.9 % CH_4, 35 % CO_2, 3.6 % C_nH_m, and 10.5 % H_2. The GY for cellulose is almost 200 mL/g. The char, gas, and tar yields for cellulose are 4.9, 40, and 55.2 wt%, respectively. The high tar yield of cellulose is due to its high volatile content (Table 1) [11]. Cellulose-based tar is a mix of anhydrosugars, like levoglucosan, furans, and carbonyls [16]. The H_2 concentration from xylan is almost double that of cellulose with 22.1 %, and its CO, CH_4, CO_2, and C_nH_m concentrations are 34.7, 5.6, 33.9, and 4 % respectively. The GY for xylan is the same as cellulose. Further, xylan gasification forms 16.9 wt% char, 41.1 wt% gas, and 42.1 wt% tar. Tar from xylan mainly contains furan and acidic compounds like furfural and acetic acid [17].

Regarding the gasification of lignin, the results differ greatly from other components. The gas from lignin is composed mainly of CO at 54.4 % and H_2 at 30.4 %, and CO_2, CH_4, and C_nH_m concentrations are 8.5, 5, and 1.9 %, respectively. The GY of lignin is 494 mL/g, which is almost 150 % higher than the GY of cellulose and xylan. Concerning the product yields, the char yield of lignin with 46.6 wt% is much higher than other components. In addition, the merely 5.1 wt% of the lignin converts to tar. Tar produced from lignin is mainly composed of phenols [16]. The higher char yield of lignin and xylan compared to cellulose is due to their branched and complicated structures which are hard to crack thus facilitate the char formation [16,38]. Further, higher amounts of fixed carbon of these components, as presented in Table 1, account for the higher char yield [11].

The results presented here suggest that the difference in gasification performance from the investigates biomass is associated with different cellulose, xylan, and lignin compositions [39]. The biomass with higher lignin content produces more syngas (hydrogen and CO) and have higher gas yield. Gasification of biomass with high xylan content produces high hydrogen with less char than lignin. However, the tar yield of xylan is much higher than lignin. The results also show that higher cellulose content results in lower hydrogen efficiency and higher tar yield, although the remaining char is much lower. The abundant aromatic rings and methoxy groups in lignin's structure suggest likely methane release during lignin decomposition [16]. Elevated methane levels enhance reforming reactions, leading to higher concentrations of H_2 and CO. Additionally, lignin's high carbon content (see Table 1) facilitates water–gas and Boudouard reactions, resulting in increased H_2 and CO production and reduced CO_2 formation [3]. This phenomenon also accounts for the greater gas yield observed during lignin

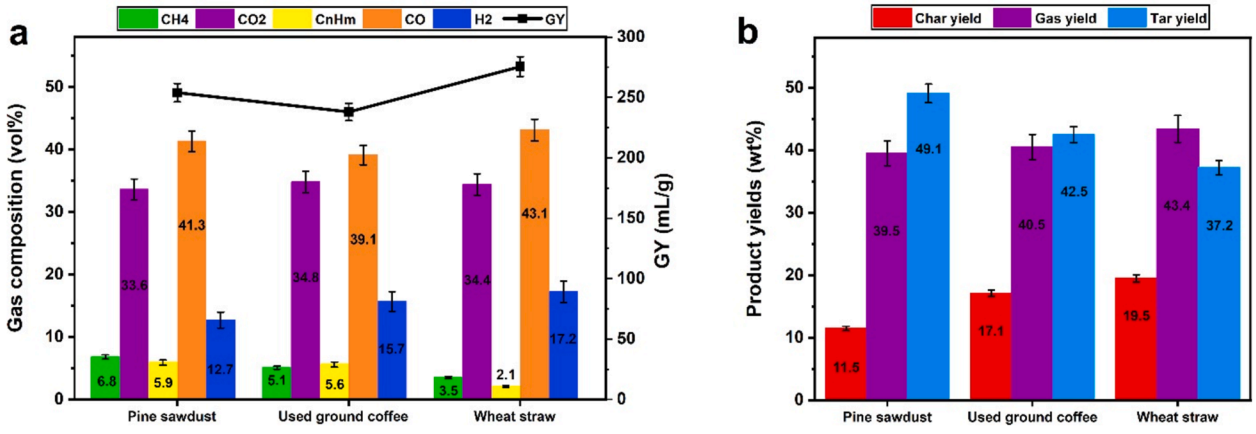

Fig. 1. Gasification results of three different biomasses a) the gas composition, and b) product yields.

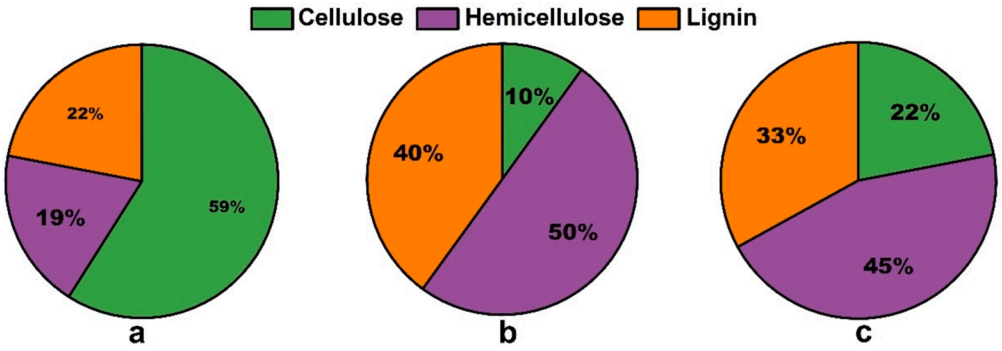

Fig. 2. The mass composition of a) pine sawdust, b) used ground coffee, and c) wheat straw.

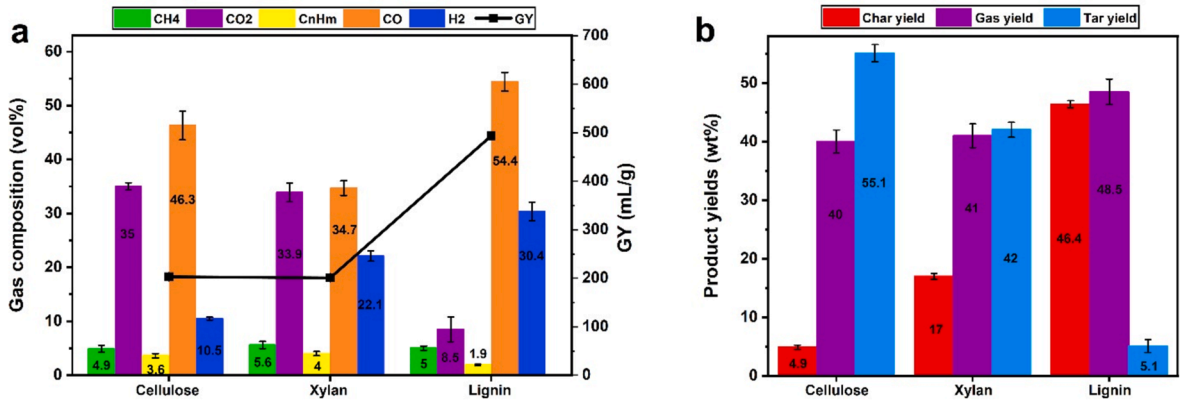

Fig. 3. Gasification results of biomass main components a) the gas composition, and b) product yields.

gasification. During the gasification of cellulose and xylan, their lower content inhibits gasification reactions, resulting in a less substantial production of H_2 and a higher proportion of CO_2 compared to lignin. The increased CO_2 content observed during the gasification of cellulose and xylan is also due to the reforming of carboxyl and acetyl groups within their structures [16]. Cellulose's susceptibility to C=O cracking makes it more likely to produce CO compared to xylan and lignin [40].

3.2. *Evaluating the interactions among biomass components*

The theoretical values for different biomass are calculated using the data for the gasification of components and biomass composition. The

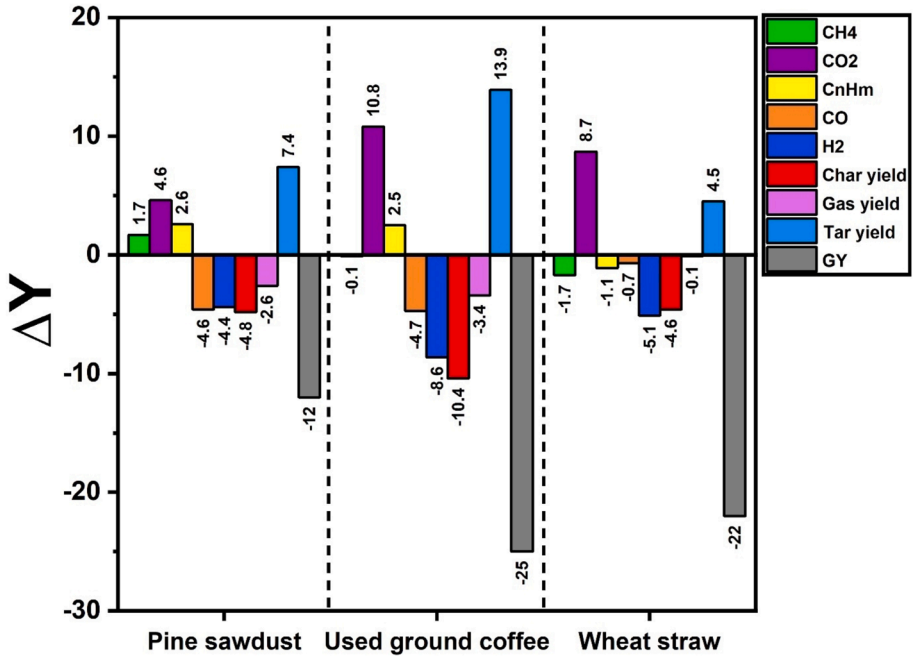

Fig. 4. The differences between experimental and theroretical gasification results.

differences between experimental and theoretical values for each response are presented in Fig. 4. The theoretical values and differences are calculated using Eq. (2) and (3) [41,42].

$$Y_{Theoretical} = aY_C + bY_H + cY_L \quad (2)$$

$$\Delta Y = Y_{Experimental} - Y_{Theoretical} \quad (3)$$

Where Y_C, Y_H, Y_L are the experimental values of cellulose, xylan, and lignin, respectively, when processed separately, and *a*, *b*, *c* are the weight fractions of cellulose, xylan, and lignin in the mixture. It should be stressed that the minus ΔY implies that the experimental value is smaller than the predicted value and vice versa.

Comparing the theoretical and experimental values in Fig. 4, it can be observed that there are discrepancies between actual and predicted results for gas composition and product yields, irrespective of the employed biomass. In all cases, the experimental CO_2 concentration and tar yield are larger than the theoretical values. However, for H_2, CO, char and gas yields, and GY, the theoretical values are larger than the actual values. For CH_4 and C_nH_m, no specific trend can be observed.

Another point worth considering is that ΔY of each response is inconsistent for all biomass. It can be deduced that the biomass composition can accurately determine ΔY. For the PS with higher cellulose content, the ΔY s are less noticeable than UGC and WS, which have more xylan and lignin. It indicates that the larger the lignin and xylan, the more interactions between biomass components can be expected since discrepancies mostly stem from the interactions among components.

As previously mentioned, differences in gas composition and product yields between experimental and theoretical results arise from interactions among biomass components. These interactions occur in both volatile-volatile and volatile-solid states [28]. Therefore, performing TGA analysis to examine the degradation patterns of individual elements and comparing these patterns between synthetic mixtures and real biomass can provide valuable insights into the possible interactions among compounds during the gasification process, especially in the volatile-solid state. The TGA analysis of the individual parts (cellulose, xylan, and lignin) was conducted to identify their degradation profiles under oxidative conditions. The mass loss profiles are compared in Fig. 5a. Further, the mass loss profiles of PS and synthetic pine sawdust are compared in Fig. 5b Fig. 5a shows that the xylan degradation occurs in two main stages. The first stage starts from 185 °C to 395 °C, in which almost 70 wt% of the sample is decomposed. This step comprises a peak at 285 °C with a left shoulder at 236 °C. The second stage, between 400 and 586 °C with a peak at 568 °C, decomposes 28 wt% of the sample. Chen et al. [16] also reported the same mass loss pattern for xylan. The decomposition of cellulose mostly occurs in a narrow range from 290 to 356 °C with a peak at 338 °C in which 85 wt% of the sample is degraded. This is due to cellulose's high volatile content and uniform unbranched crystalline chemical structure [17]. There is also a small peak between 452 to 510 °C for cellulose, relating to the further degradation of solid residues from the previous step [11]. By 500 and 600 °C, cellulose and xylan are fully decomposed, respectively. However, the lignin decomposition profile is wide, indicating its stable structure and complex degradation mechanism compared to cellulose and xylan [38,43]. The lignin decomposition starts at 145 °C and consists of several steps, with the main peak happening at a higher temperature of around 778 °C. There is also a small peak for lignin between 145 and 318 °C. Notably, between 525 and 775 °C, no mass loss can be seen in the lignin profile. By 800 °C, 56 wt% of the lignin is converted, and the remaining indicates the weight of highly stable aromatics that can be the precursor of char formation [17]. Chen et al. [16] correlate the differences in biomass components' thermal decomposition behaviour to their dissimilar

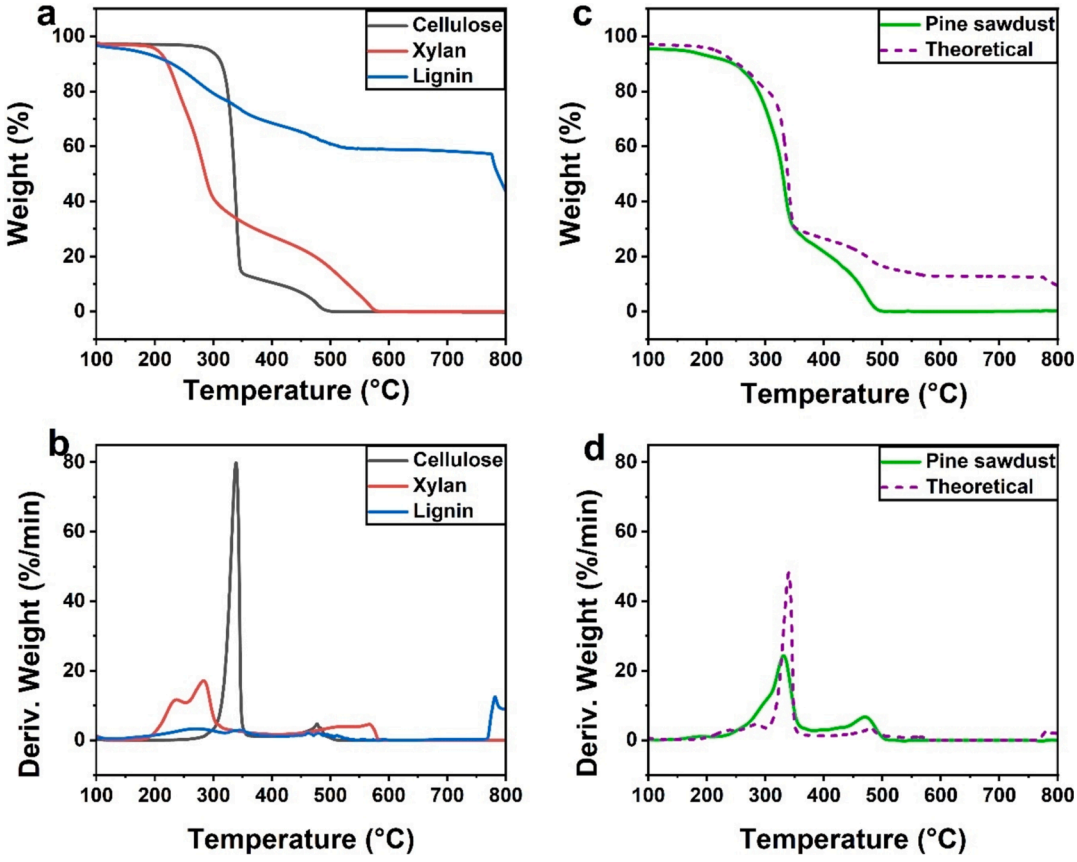

Fig. 5. Thermal decomposition profiles (a, b) for neat xylan, cellulose, and lignin and the comparison between theoretical and experimental TGA and DTG profiles for actual and synthetic pine sawdust (c, d).

chemical structures. Lignin and xylan with more complex structure needs a higher activation energy for decomposition than cellulose [16]. The results observed here agree with the literature concerning the decomposition of biomass components [11,12,16,17,43].

Fig. 5b compares the TGA and DTG figures of pine and synthetic pine. These figures are different, particularly when the temperature exceeds 300 °C. The interactions among biomass components can mainly account for mass loss profile differences [44]. Below 300 °C, the degradation of pine is more accelerated than that of synthetic pine. In this region, the degradation of cellulose has not started yet; thus, the xylan-lignin interaction causes the variations. When the temperature reaches 350 °C, close to the DTG_{max} of cellulose, the differences between actual and theoretical degradation figures become more significant and real pine decomposes much quicker. Since the decompositions of xylan and lignin are not completed until high temperatures, cellulose-lignin and cellulose-xylan interactions (volatile-volatile or volatile-char) can be significant in this temperature region.

Consequently, all interactions can be important, and the biomass composition can determine the most influential ones. This observation can support the findings that the ΔY is larger for the biomass with higher lignin content and smaller for biomass with higher cellulose content. When the cellulose content is high, the overlapping region between components is limited since cellulose decomposition occurs in narrow region, thus, fewer interactions are expected. However, more interactions are expected at higher lignin and xylan contents because of wider overlapping areas. The overlapping of degradation regions is required for the emergence of interactions among biomass components through thermal degradation [8,12]. It is worth noting that the role of physical and chemical hydrogen and covalent bonds among components, which need energy for dissociation [12], the effects of mineral matter and other elements, like starch, protein, and extractives [11] can be other reasons why artificial biomass fails to mimic the degradation behaviour of natural biomass.

Lignin is composed of three main structural units: p-hydroxyphenyl, guaiacyl, and syringyl [23]. Its characteristics vary significantly based on the type and source of the biomass [14]. Softwood lignin is mainly composed of guaiacyl units, while hardwood lignin includes a mix of guaiacyl and syringyl units [23]. In this study, the lignin used is sourced from hardwood, containing both guaiacyl and syringyl units. Additionally, the cellulose properties can vary depending on the source [45]. This study uses microcrystalline cellulose from cotton linters. It is important to note that using different types of lignin and cellulose may potentially affect the results, which represents an opportunity for future research. Assessing the impact of other biomass components, such as moisture, alkali and alkaline earth metals (AAEMs), proteins, lipids, waxes, and nitrogenous compounds, on the possible interactions, as well as the predictability of various biomass gasification performances, is also a further avenue for future studies. Additionally, conducting several characterizations related to the elemental composition and chemical structure of the remaining char would provide valuable insights into the nature of interactions between biomass components. This can be explored in future studies. Exploring the predictability of gasification results with a broader range of biomass in the future works can further validate and consolidate the findings presented in this study.

4. Conclusion

In this study, the gasification of three biomass, pine sawdust (PS), used ground coffee (UGC), and wheat straw (WS), was compared under the same condition. UGC and WS were found to produce more hydrogen and less tar but higher amounts of char. The biomass composition analysis of hemicellulose, cellulose, and lignin indicated that PS has high cellulose while UGC and WS are rich in hemicellulose and lignin. The differences in the gas composition and product yields between the three biomass samples were correlated with the differences in biomass composition. To assess the effects of each element on the process, the gasification of cellulose, xylan as the representative of hemicellulose, and lignin were carried out individually. It was found that the gas from lignin is rich in H_2 and CO while cellulose produces CO and CO_2, and its H_2 concentration of 10.5 % is lower than lignin with 30.4 %. Concerning the product yields, it was found that the gas yield for cellulose is less than lignin, where cellulose mostly converts to tar at 55.1 %, while its char yield is 4.9 %. However, lignin's char yield is high at 46.4 %, but its tar yield is only 5.1 %. Xylan shows a characteristic in-between cellulose and lignin in gas composition and product yields. Comparison of experimental and theoretical values for three biomass samples and observed dissimilarities, it was concluded that the interactions between components occur through the process. The degradation profiles of individual components were assessed, and TGA and DTG curves of actual PS were compared with the theoretical figures to gain insight into the source of these interactions. It was found that xylan-lignin, cellulose-xylan, and cellulose-lignin interactions can be significant due to the overlapping degradation region, and the biomass composition can determine the most effective type of interactions. It was concluded that when cellulose content is high, the overlapping region becomes smaller with fewer interactions and vice versa. Integrating TGA results with the dissimilarities quantification results, ΔY, demonstrated that the predicted and actual results are more similar if the biomass has a high cellulose content. The ΔY becomes larger, and the predicted results are less reliable when biomass has high lignin and xylan contents.

CRediT authorship contribution statement

Mojtaba Ajorloo: Writing – original draft, Validation, Methodology, Investigation, Formal analysis, Data curation, Conceptualization. **Maryam Ghodrat:** Writing – review & editing, Supervision, Resources, Project administration, Funding acquisition. **Jason Scott:** Writing – review & editing, Supervision, Resources, Project administration, Methodology, Funding acquisition. **Vladimir Strezov:** Writing – review & editing, Supervision, Resources, Project administration, Funding acquisition.

Declaration of competing interest

The authors declare that they have no known competing financial interests or personal relationships that could have appeared to influence the work reported in this paper.

Data availability

No data was used for the research described in the article.

References

[1] Kombe EY, Lang'at N, Njogu P, Malessa R, Weber C-T, Njoka F, et al. Process modeling and evaluation of optimal operating conditions for production of hydrogen-rich syngas from air gasification of rice husks using aspen plus and response surface methodology. Bioresour Technol 2022;361:127734. https://doi.org/10.1016/j.biortech.2022.127734.

[2] Shen Y. Biomass pretreatment for steam gasification toward H2-rich syngas production – An overview. Int J Hydrogen Energy 2024;66:90–102. https://doi.org/10.1016/j.ijhydene.2024.04.096.

[3] Li H, Hu Y, Wang H, Han X, El-Sayed H, Zeng Y, et al. Supercritical water gasification of lignocellulosic biomass: Development of a general kinetic model for prediction of gas yield. Chem Eng J 2022;433:133618. https://doi.org/10.1016/j.cej.2021.133618.

[4] Ajorloo M, Ghodrat M, Scott J, Strezov V. Recent advances in thermodynamic analysis of biomass gasification: A review on numerical modelling and simulation. J Energy Inst 2022;102:395–419. https://doi.org/10.1016/j.joei.2022.05.003.

[5] Meryemoglu B, Kaya Ozsel B, Irmak S. Evaluation of hardwood or softwood bark biomass as feed materials for aqueous-phase reforming gasification process. Int J Hydrogen Energy 2024;53:1044–51. https://doi.org/10.1016/j.ijhydene.2023.12.104.

[6] Mishra K, Singh Siwal S, Kumar Saini A, Thakur VK. Recent update on gasification and pyrolysis processes of lignocellulosic and algal biomass for hydrogen production. Fuel 2023;332:126169. https://doi.org/10.1016/j.fuel.2022.126169.

[7] Chen R, Zhang S, Cong K, Li Q, Zhang Y. Insight into synergistic effects of biomass-polypropylene co-pyrolysis using representative biomass constituents. Bioresour Technol 2020;307:123243. https://doi.org/10.1016/j.biortech.2020.123243.
[8] Kumar R, Strezov V, Weldekidan H, He J, Singh S, Kan T, et al. Lignocellulose biomass pyrolysis for bio-oil production: A review of biomass pre-treatment methods for production of drop-in fuels. Renew Sustain Energy Rev 2020;123:109763. https://doi.org/10.1016/j.rser.2020.109763.
[9] Coker EN, Lujan-Flores X, Donaldson B, Yilmaz N, Atmanli A. An Assessment of the conversion of biomass and industrial waste products to activated carbon. Energies (Basel) 2023;16:1606. https://doi.org/10.3390/en16041606.
[10] Sarker TR, Nanda S, Meda V, Dalai AK. Process optimization and investigating the effects of torrefaction and pelletization on steam gasification of canola residue. Fuel 2022;323:124239. https://doi.org/10.1016/j.fuel.2022.124239.
[11] Cao W, Li J, Martí-Rosselló T, Zhang X. Experimental study on the ignition characteristics of cellulose, hemicellulose, lignin and their mixtures. J Energy Inst 2019;92:1303–12. https://doi.org/10.1016/j.joei.2018.10.004.
[12] Yu J, Paterson N, Blamey J, Millan M. Cellulose, xylan and lignin interactions during pyrolysis of lignocellulosic biomass. Fuel 2017;191:140–9. https://doi.org/10.1016/j.fuel.2016.11.057.
[13] Wu Y, Wu S, Zhang H, Xiao R. Cellulose-lignin interactions during catalytic pyrolysis with different zeolite catalysts. Fuel Process Technol 2018;179:436–42. https://doi.org/10.1016/j.fuproc.2018.07.027.
[14] Ferreiro AI, Ferreira AF, Fernandes EC, Coelho P. Influence of process parameters on biomass gasification: A review of experimental studies in entrained flow reactors and droptube furnaces. Biomass Bioenergy 2024;185:107217. https://doi.org/10.1016/j.biombioe.2024.107217.
[15] Wang J, Jiang H, Chen Y, Han Y, Cai J, Peng Y, et al. Emission characteristics and influencing mechanisms of PAHs and EC from the combustion of three components (cellulose, hemicellulose, lignin) of biomasses. Sci Total Environ 2023;859:160359. https://doi.org/10.1016/j.scitotenv.2022.160359.
[16] Chen D, Cen K, Zhuang X, Gan Z, Zhou J, Zhang Y, et al. Insight into biomass pyrolysis mechanism based on cellulose, hemicellulose, and lignin: Evolution of volatiles and kinetics, elucidation of reaction pathways, and characterization of gas, biochar and bio-oil. Combust Flame 2022;242:112142. https://doi.org/10.1016/j.combustflame.2022.112142.
[17] Chen W-H, Wang C-W, Ong HC, Show PL, Hsieh T-H. Torrefaction, pyrolysis and two-stage thermodegradation of hemicellulose, cellulose and lignin. Fuel 2019;258:116168. https://doi.org/10.1016/j.fuel.2019.116168.
[18] Almagro-Herrera N, Lozano-Calvo S, Palma A, García JC, Díaz MJ. Assessing the influence of biomass origin and fractionation methods on pyrolysis of primary biomass fractions. Fuel 2024;367:131501. https://doi.org/10.1016/j.fuel.2024.131501.
[19] Anand A, Gautam S, Chand RL. A characteristic-based decision tree approach for sustainable energy applications of biomass residues from two major classes. Fuel 2023;339:127483. https://doi.org/10.1016/j.fuel.2023.127483.
[20] Ge L, Zhao C, Zuo M, Du Y, Tang J, Chu H, et al. Effects of Fe addition on pyrolysis characteristics of lignin, cellulose and hemicellulose. J Energy Inst 2023;107:101177. https://doi.org/10.1016/j.joei.2023.101177.
[21] Zhang S, Wu M, Qian Z, Li Q, Zhang Y, Zhou H. CO rich syngas production from catalytic CO2 gasification-reforming of biomass components on Ni/CeO2. Fuel 2024;357:130087. https://doi.org/10.1016/j.fuel.2023.130087.
[22] Kim JY, Kim D, Li ZJ, Dariva C, Cao Y, Ellis N. Predicting and optimizing syngas production from fluidized bed biomass gasifiers: A machine learning approach. Energy 2023;263:125900. https://doi.org/10.1016/j.energy.2022.125900.
[23] Pang Y, Zhu X, Li N, Wang Z. Investigation on reaction mechanism for CO2 gasification of softwood lignin by ReaxFF MD method. Energy 2023;267:126533. https://doi.org/10.1016/j.energy.2022.126533.
[24] Samani N, Khalil R, Seljeskog M, Bakken J, Thapa RK, Eikeland MS. Experimental and simulation studies of oxygen-blown, steam-injected, entrained flow gasification of lignin. Fuel 2024;362:130713. https://doi.org/10.1016/j.fuel.2023.130713.
[25] Song G, Huang D, Ren Q, Hu S, Xu J, Xu K, et al. Inner-particle reaction mechanism of cellulose, hemicellulose and lignin during photo-thermal pyrolysis process: Evolution characteristics of free radicals. Energy 2024;297:131201. https://doi.org/10.1016/j.energy.2024.131201.
[26] Zhang S, Wu M, Bie X, Qian Z, Li Q, Zhang Y, et al. Deciphering interactions between biomass components during CO2 gasification: Insights from thermogravimetric behavior, gas production, and char reactivity. Fuel 2024;371:131974. https://doi.org/10.1016/j.fuel.2024.131974.
[27] Zhu J, Du C. Interaction between lignin and cellulose during the pyrolysis process. Int J Biol Macromol 2024;265:131093. https://doi.org/10.1016/j.ijbiomac.2024.131093.
[28] Xue P, Liu M, Yang H, Zhang H, Chen Y, Hu Q, et al. Mechanism study on pyrolysis interaction between cellulose, hemicellulose, and lignin based on photoionization time-of-flight mass spectrometer (PI-TOF-MS) analysis. Fuel 2023;338:127276. https://doi.org/10.1016/j.fuel.2022.127276.
[29] Fermoso J, Mašek O. Thermochemical decomposition of coffee ground residues by TG-MS: A kinetic study. J Anal Appl Pyrolysis 2018;130:358–67. https://doi.org/10.1016/j.jaap.2017.12.007.
[30] Chang G, Huang Y, Xie J, Yang H, Liu H, Yin X, et al. The lignin pyrolysis composition and pyrolysis products of palm kernel shell, wheat straw, and pine sawdust. Energy Convers Manag 2016;124:587–97. https://doi.org/10.1016/j.enconman.2016.07.038.
[31] Carrier M, Loppinet-Serani A, Denux D, Lasnier J-M, Ham-Pichavant F, Cansell F, et al. Thermogravimetric analysis as a new method to determine the lignocellulosic composition of biomass. Biomass Bioenergy 2011;35:298–307. https://doi.org/10.1016/j.biombioe.2010.08.067.
[32] Ayeni AO, Hymore FK, Mudliar SN, Deshmukh SC, Satpute DB, Omoleye JA, et al. Hydrogen peroxide and lime based oxidative pretreatment of wood waste to enhance enzymatic hydrolysis for a biorefinery: Process parameters optimization using response surface methodology. Fuel 2013;106:187–94. https://doi.org/10.1016/j.fuel.2012.12.078.
[33] Wang H, Han X, Zeng Y, Xu CC. Development of a global kinetic model based on chemical compositions of lignocellulosic biomass for predicting product yields from hydrothermal liquefaction. Renew Energy 2023;215:118956. https://doi.org/10.1016/j.renene.2023.118956.
[34] Mohabeer C, Reyes L, Abdelouahed L, Marcotte S, Taouk B. Investigating catalytic de-oxygenation of cellulose, xylan and lignin bio-oils using HZSM-5 and Fe-HZSM-5. J Anal Appl Pyrolysis 2019;137:118–27. https://doi.org/10.1016/j.jaap.2018.11.016.
[35] Ajorloo M, Ghodrat M, Scott J, Strezov V. Modelling and statistical analysis of plastic biomass mixture co-gasification. Energy 2022;256:124638. https://doi.org/10.1016/j.energy.2022.124638.
[36] Raheem A, Abbasi SA, Mangi FH, Ahmed S, He Q, Ding L, et al. Gasification of algal residue for synthesis gas production. Algal Res 2021;58:102411. https://doi.org/10.1016/j.algal.2021.102411.
[37] Ghodke PK, Sharma AK, Jayaseelan A, Gopinath KP. Hydrogen-rich syngas production from the lignocellulosic biomass by catalytic gasification: A state of art review on advance technologies, economic challenges, and future prospectus. Fuel 2023;342:127800. https://doi.org/10.1016/j.fuel.2023.127800.
[38] Zong P, Jiang Y, Tian Y, Li J, Yuan M, Ji Y, et al. Pyrolysis behavior and product distributions of biomass six group components: Starch, cellulose, hemicellulose, lignin, protein and oil. Energy Convers Manag 2020;216:112777. https://doi.org/10.1016/j.enconman.2020.112777.
[39] Nguyen VG, Nguyen-Thi TX, Phong Nguyen PQ, Tran VD, Ağbulut Ü, Nguyen LH, et al. Recent advances in hydrogen production from biomass waste with a focus on pyrolysis and gasification. Int J Hydrogen Energy 2024;54:127–60. https://doi.org/10.1016/j.ijhydene.2023.05.049.
[40] Li A, Han H, Zheng K, Zhu M, Xu K, Xu J, et al. Sludge pyrolysis integrated biomass gasification to promote syngas: Comparison of different biomass. Sci Total Environ 2024;908:168278. https://doi.org/10.1016/j.scitotenv.2023.168278.
[41] Gu J, Fan H, Wang Y, Zhang Y, Yuan H, Chen Y. Co-pyrolysis of xylan and high-density polyethylene: Product distribution and synergistic effects. Fuel 2020;267:116896. https://doi.org/10.1016/j.fuel.2019.116896.
[42] Ajorloo M, Ghodrat M, Scott J, Strezov V. Experimental analysis of the effects of feedstock composition on the plastic and biomass Co-gasification process. Renew Energy 2024;231:120960. https://doi.org/10.1016/j.renene.2024.120960.
[43] Kuo P-C, Sun Z, Özdemir F, Aziz M, Wu W. CO2 utilization in chemical looping gasification and co-gasification of lignocellulosic biomass components over iron-based oxygen carriers: Thermogravimetric behavior, synergistic effect, and reduction characteristics. J Environ Chem Eng 2023;11:109971. https://doi.org/10.1016/j.jece.2023.109971.
[44] Batuer A, Long J, Du H, Chen D. Multi-products oriented co-pyrolysis of papers, plastics, and textiles in MSW and the synergistic effects. J Anal Appl Pyrolysis 2022;163:105478. https://doi.org/10.1016/j.jaap.2022.105478.
[45] González Martínez M, Marlin N, Da Silva PD, Dupont C, del Mar Saavedra Rios C, Meyer X-M, et al. Impact of cellulose properties on its behavior in torrefaction: commercial microcrystalline cellulose versus cotton linters and celluloses extracted from woody and agricultural biomass. Cellul 2021;28:4761–79. https://doi.org/10.1007/s10570-021-03812-y.